J. Fluid Mech. (1986), *vol.* 168, *pp.* 457–478
Printed in Great Britain

Bubble dynamics in a compressible liquid. Part 1. First-order theory

By A. PROSPERETTI† AND A. LEZZI†
Dipartimento di Fisica, Universitá degli Studi, 20133, Milano, Italy

(Received 9 October 1985)

The radial dynamics of a spherical bubble in a compressible liquid is studied by means of a simplified singular-perturbation method to first order in the bubble-wall Mach number. It is shown that, at this order, a one-parameter family of approximate equations for the bubble radius exists, which includes those previously derived by Herring and Keller as special cases. The relative merits of these and other equations of the family are judged by comparison with numerical results obtained from the complete partial-differential-equation formulation by the method of characteristics. It is concluded that an equation close to the Keller form, but written in terms of the enthalpy of the liquid at the bubble wall, rather than the pressure, is most accurate, at least for the cases considered of collapse in a constant-pressure field and collapse driven by a Gaussian pressure pulse. A physical discussion of the magnitude and nature of compressibility effects is also given.

1. Introduction

In the present and in a companion paper (Lezzi & Prosperetti 1986, hereafter referred to as II), we propose to give a systematic approximate theory of the radial motion of a spherical bubble in a compressible liquid in the absence of boundaries. This problem, which was first considered in connection with underwater explosions (Herring 1941; Cole 1948; Trilling 1952; Keller & Kolodner 1956), has recently been revived by impressive improvements in ultra-high-speed cinematography and holocinematography (Lauterborn & Vogel 1984) which has rendered the detailed experimental investigation of cavitation-bubble collapse possible. Furthermore, liquid compressibility causes radiation damping, which influences important characteristics of nonlinear forced oscillatory motion such as period doubling and transition to chaos. In view of the recent interest in these questions (Lauterborn & Suchla 1984; Lauterborn 1983, 1985) it is desirable to have an equation of motion for the bubble boundary as realistic as possible in this as in other respects.

In addition to the classic studies already cited, a number of papers have appeared in the last few years addressing the same problem (Jahsman 1968; Epstein & Keller 1971; Flynn 1975; Tomita & Shima 1977; Lastman & Wentzell 1979, 1981; Fujikawa & Akamatsu 1980; Cramer 1980; Rath 1980; Tilmann 1980; Keller & Miksis 1980). Several different approximate equations now exist with no clear relationship to each other. The present study was undertaken to clarify the situation by placing the treatment of the problem in the framework of a systematic perturbation method. In this way we show that entire *families* of equations exist having the same degree of accuracy and therefore entirely equivalent on formal grounds. This situation is

† Present address: Department of Mechanical Engineering, The Johns Hopkins University, Baltimore, MD 21218, USA.

reminiscent of that found in the modelling of long surface waves in shallow water (see, e.g., Whitham 1974). In particular we find that the Herring and Keller equations are different members of the first-order family of equations.

The question of which member of each family is 'best' cannot be answered in absolute terms. We have solved the complete partial differential formulation of the problem numerically in some cases to compare the results with the predictions of some members of the families of equations. To first order we conclude that an equation close to the Keller form is accurate in the cases examined.

In the present paper we consider the acoustic correction to the incompressible Rayleigh–Plesset equation (see, e.g., Plesset & Prosperetti 1977). Use is made of a rather heuristic version of the method of matched asymptotic expansions in which the small parameter is the bubble-wall Mach number. In II we carry the analysis one step further to second order, and use a more rigorous version of the perturbation method. The motivation is not only the desire to put the results of the present paper on a sounder basis, but the difficulty into which the heuristic perturbation procedure runs at the next step. The subdivision of material between the two papers also enables us to render the present one more readable and physically intelligible. To enhance these features we include in §3 a qualitative discussion of our approach and results.

The extreme violence of bubble motion in some cases is well known and equations valid to first order in the Mach number cannot be expected to have general validity. However, a bubble collapsing with a radial velocity comparable with the speed of sound of the liquid or greater in most cases will shatter at the end of the collapse so that the rebound phase of the motion, where the liquid compressibility is most prominent, will be absent. Our results can therefore be useful in practically all situations in which the bubble maintains its integrity without significant distortion of the spherical shape. In addition, as shown in II, the present first-order correction to the incompressible results captures to a large extent the effect of compressibility, with the next term having only a minor influence.

2. Mathematical formulation

With the assumption of spherical symmetry the motion of the liquid is governed by the equation of continuity

$$\frac{\partial \rho}{\partial t} + \nabla \cdot (\rho \boldsymbol{u}) = 0, \tag{2.1}$$

and momentum

$$\frac{\partial u}{\partial t} + u \frac{\partial u}{\partial r} + \frac{1}{\rho} \frac{\partial p}{\partial r} = 0, \tag{2.2}$$

where $\mathbf{u} = u\hat{\boldsymbol{r}}$ is the velocity field entirely directed in the radial direction and the other symbols have their customary meaning. In bubble dynamics, high-speed motions such that liquid compressibility is important usually occur only when thermal effects in the liquid are unimportant (Plesset & Prosperetti 1977). Therefore the liquid state is completely defined by a single thermodynamic variable, which permits the introduction of a speed of sound c and enthalpy h through the definitions

$$\frac{\mathrm{d}p}{\mathrm{d}\rho} = c^2, \quad h = \int_{p_\infty}^{p} \frac{\mathrm{d}p}{\rho}. \tag{2.3}$$

Here the reference pressure p_∞ is chosen as the pressure in the undisturbed liquid. Furthermore, since a purely radial motion is evidently irrotational, we may introduce

a velocity potential φ such that $u = \partial\varphi/\partial r$. With these definitions (2.1) may be rewritten as

$$\frac{1}{c^2}\left(\frac{\partial h}{\partial t}+u\frac{\partial h}{\partial r}\right)+\nabla^2\varphi = 0, \tag{2.4}$$

while (2.2) may be integrated once to give

$$\frac{\partial\varphi}{\partial t}+\tfrac{1}{2}u^2+h = 0. \tag{2.5}$$

In obtaining this equation the fluid at infinity has been assumed to be undisturbed and the time derivative of φ has been taken to vanish there.

To complete the mathematical formulation we need the kinematic boundary condition at the bubble wall $r = R(t)$,

$$u(r = R(t), t) = \frac{\mathrm{d}R}{\mathrm{d}t}, \tag{2.6}$$

and the condition on the normal stresses, which is

$$p_B(t) = p_{\mathrm{i}}(t)-\frac{1}{R}\left(2\sigma+4\mu\frac{\mathrm{d}R}{\mathrm{d}t}\right). \tag{2.7}$$

Here $p_B(t) = p(R(t), t)$ is the pressure on the liquid side of the interface, σ is the surface tension, and μ is the liquid viscosity. The internal pressure p_{i} should in general be determined from a consideration of the conservation equations inside the bubble. The assumption that the liquid remains isothermal effectively uncouples the internal and the external problems, and for the time being p_{i} can be regarded as given.

In (2.7) we retain the liquid viscosity although it has been dropped in (2.2). The justification is that in the momentum equation viscous effects only enter through their coupling with the compressibility of the liquid and therefore are ordinarily small. They have been included by Keller & Miksis (1980). In (2.6) some small terms due to mass exchange at the interface have been neglected. These effects, which are quite small, have been considered by Fujikawa & Akamatsu (1980) for the case of free motion of the bubble.

In the following, explicit expressions for c and h will be needed. To this end we make use of an equation of state of the modified Tait form

$$\frac{p+B}{p_\infty+B} = \left(\frac{\rho}{\rho_\infty}\right)^n. \tag{2.8}$$

The values $B = 3049.13$ bars, $n = 7.15$ given an excellent fit to the experimental pressure–density relation for water up to 10^5 bars (Fujikawa & Akamatsu 1980) and are used in the numerical examples of this paper and of II. With (2.8) we readily find the following relations:

$$c^2 = \frac{n(p+B)}{\rho}, \tag{2.9}$$

$$h = \frac{c^2-c_\infty^2}{n-1}, \tag{2.10}$$

where $c_\infty^2 = n(p_\infty+B)/\rho_\infty$ is the undisturbed speed of sound, squared, in the liquid.

3. Preliminary considerations

We propose to give now a heuristic discussion of the key features of the present problem which will serve to clarify the following developments and naturally lead to the singular perturbation methods applied here and in II.

When the pressure in the liquid does not deviate too strongly from p_∞ we may write, using the definition (2.3) of c,

$$h = \int_{p_\infty}^{p} \left(\frac{1}{\rho_\infty} - \frac{p'-p_\infty}{\rho_\infty^2 c_\infty^2} + \dots \right) \mathrm{d}p'$$

$$= \frac{p-p_\infty}{\rho_\infty} \left(1 - \frac{1}{2} \frac{p-p_\infty}{\rho_\infty c_\infty^2} + \dots \right), \tag{3.1}$$

and, similarly,

$$c^{-2} = c_\infty^{-2} \left(1 - \frac{B}{A} \frac{p-p_\infty}{\rho_\infty c_\infty^2} + \dots \right), \tag{3.2}$$

where $(B/A) = 2\rho_\infty c_\infty (\mathrm{d}c/\mathrm{d}p)_\infty$ is the standard nonlinearity parameter of acoustics. Upon substitution into (2.4) one finds

$$\nabla^2 \varphi + \frac{1}{\rho_\infty c_\infty^2} \left(\frac{\partial p}{\partial t} + u \frac{\partial p}{\partial r} \right) \left[1 - \left(1 + \frac{B}{A} \right) \frac{p-p_\infty}{\rho_\infty c_\infty^2} + \dots \right] = 0, \tag{3.3}$$

while (2.5) gives

$$\frac{\partial \varphi}{\partial t} + \tfrac{1}{2} u^2 + \frac{p-p_\infty}{\rho_\infty} \left(1 - \frac{p-p_\infty}{2\rho_\infty c_\infty^2} + \dots \right) = 0. \tag{3.4}$$

As $c_\infty \to \infty$ the standard incompressible formulation is recovered, namely

$$\nabla^2 \varphi = 0, \quad \frac{\partial \varphi}{\partial t} + \tfrac{1}{2} u^2 + \frac{p-p_\infty}{\rho_\infty} = 0. \tag{3.5a,b}$$

This formulation differs from the exact one (3.3), (3.4) because it disregards two physical effects, the finite speed of propagation of pressure waves, and the compression energy stored in the liquid through a change of its specific volume (second and higher terms in (3.1)). It may be expected that both effects will be unimportant near the bubble, the first one because propagation times are much shorter than the timescale T for the motion of the boundary, the second one because the kinetic energy and the 'pressure energy' (first term in (3.1)) are large in this region. Hence the incompressible formulation (3.5) is expected to be accurate near the bubble. Far from the bubble, on the other hand, the finite speed of propagation is essential. However, the amplitude of the motion caused by the bubble is much attenuated so that (3.3) and (3.4) can be linearized with a negligible error,

$$\nabla^2 \varphi + \frac{1}{\rho_\infty c_\infty^2} \frac{\partial p}{\partial t} = 0, \quad \frac{\partial \varphi}{\partial t} + \frac{p-p_\infty}{\rho_\infty} = 0. \tag{3.6a,b}$$

This is the standard acoustic formulation from which the wave equation for the potential

$$\nabla^2 \varphi - \frac{1}{c_\infty^2} \frac{\partial^2 \varphi}{\partial t^2} = 0 \tag{3.7}$$

immediately follows. It is clear that, in this context, 'far from the bubble' means at distances r of the order

$$r \approx c_\infty T, \tag{3.8}$$

while 'near the bubble' means at distances of the order

$$r \approx R_0, \tag{3.9}$$

where R_0 is of the order of the bubble radius. In practical applications the ratio of the two scales,

$$\epsilon = \frac{R_0}{c_\infty T}, \tag{3.10}$$

is a small parameter so that the near and the far field are well separated and the problem may be viewed as a singular perturbation one.

Keller (Keller & Kolodner 1956; Epstein & Keller 1972; Keller & Miksis 1980) used a formulation consisting of the wave equation (3.7) and the incompressible Bernoulli integral (3.5*b*) to derive an approximate equation of motion for the bubble radius. The reasons for the success of this procedure are evident from the above considerations. The wave equation is accurate in the far field, while in the near field it differs from Laplace's equation (3.5*a*) by an unimportant term. Similarly, the Bernoulli integral (3.5*b*) is accurate in the near field and differs from the appropriate far-field relation (3.6*b*) by the term $\frac{1}{2}u^2$ which is small in that region. On the basis of this approximate formulation Keller and co-workers obtained the following approximate equation:

$$\left(1-c_\infty^{-1}\frac{\mathrm{d}R}{\mathrm{d}t}\right)R\frac{\mathrm{d}^2R}{\mathrm{d}t^2}+\frac{3}{2}\left(1-\tfrac{1}{3}c_\infty^{-1}\frac{\mathrm{d}R}{\mathrm{d}t}\right)\left(\frac{\mathrm{d}R}{\mathrm{d}t}\right)^2$$
$$=\left(1+c_\infty^{-1}\frac{\mathrm{d}R}{\mathrm{d}t}\right)\frac{1}{\rho_\infty}\left[p_B(t)-p_\infty-p_{\mathrm{v}}\left(t+\frac{R}{c_\infty}\right)\right]+\frac{R}{\rho_\infty c_\infty}\frac{\mathrm{d}p_B(t)}{\mathrm{d}t}, \tag{3.11}$$

where $p_{\mathrm{v}}(t)$ denotes the variable part of the pressure in the liquid at the location of the bubble centre in the absence of the bubble. It will be shown in the following that this equation is correct to first order in the Mach number of the bubble-wall motion, i.e. that the error term has the order $(c_\infty^{-1}\,\mathrm{d}R/\mathrm{d}t)^2$. For $c_\infty \to \infty$ (3.11) reduces to the well-known Rayleigh–Plesset equation of incompressible bubble dynamics

$$R\frac{\mathrm{d}^2R}{\mathrm{d}t^2}+\frac{3}{2}\left(\frac{\mathrm{d}R}{\mathrm{d}t}\right)^2=\frac{1}{\rho_\infty}[p_B(t)-p_\infty-p_{\mathrm{v}}(t)], \tag{3.12}$$

which therefore has an error of order $(c_\infty^{-1}\,\mathrm{d}R/\mathrm{d}t)$. The estimates given of the error terms show that if, for example, (3.12) is multiplied by $(c_\infty^{-1}\,\mathrm{d}R/\mathrm{d}t)$ and subtracted from (3.11) the result will have the same degree of accuracy as (3.11). The equation found by this procedure is

$$\left(1-2c_\infty^{-1}\frac{\mathrm{d}R}{\mathrm{d}t}\right)R\frac{\mathrm{d}^2R}{\mathrm{d}t^2}+\frac{3}{2}\left(1-\tfrac{4}{3}c_\infty^{-1}\frac{\mathrm{d}R}{\mathrm{d}t}\right)\left(\frac{\mathrm{d}R}{\mathrm{d}t}\right)^2$$
$$=\frac{1}{\rho_\infty}\left[p_B(t)-p_\infty-p_{\mathrm{v}}\left(t+\frac{R}{c_\infty}\right)+\frac{R}{c_\infty}\frac{\mathrm{d}p_B(t)}{\mathrm{d}t}\right], \tag{3.13}$$

and was originally derived by Herring (1941); see also Trilling (1952). Clearly a whole one-parameter family of equations can be obtained in this way combining (3.11) and (3.12). From the mathematical viewpoint, which member of the family has the least error is of course a meaningless question because all of them can legitimately be applied only when $(c_\infty^{-1}\,\mathrm{d}R/\mathrm{d}t)^2$ is negligibly small. However, the question has a considerable practical importance because one would like to have an equation sufficiently robust to be approximately applicable even outside its strict domain of validity. Unfortunately, it does not appear possible to settle this matter other than

by comparison of the equations with numerical solutions of the original partial differential formulation. This will be attempted later in the paper, although the consideration of only a few specific cases can only give limited answers. As will be shown in II, the same ambiguity arises at the next step in the perturbation solution of the problem, where a two-parameter family of equations is found.

An equation similar to (3.11) was proposed by Gilmore (1952) on the basis of the Kirkwood–Bethe approximation (1942; see also Cole 1948), and is

$$\left(1-C^{-1}\frac{\mathrm{d}R}{\mathrm{d}t}\right)R\frac{\mathrm{d}^2R}{\mathrm{d}t^2}+\frac{3}{2}\left(1-\tfrac{1}{3}C^{-1}\frac{\mathrm{d}R}{\mathrm{d}t}\right)\left(\frac{\mathrm{d}R}{\mathrm{d}t}\right)^2 = \left(1+C^{-1}\frac{\mathrm{d}R}{\mathrm{d}t}\right)H+\left(1-C^{-1}\frac{\mathrm{d}R}{\mathrm{d}t}\right)\frac{R}{C}\frac{\mathrm{d}H}{\mathrm{d}t}. \quad (3.14)$$

Here C and H denote the values of the speed of sound and of the enthalpy at the bubble surface, computed from the exact relations (2.3). Since in (3.11) one can approximately set $p_{\mathrm{v}}(t+R/c_\infty)\approx p_{\mathrm{v}}(t)+(R/c_\infty)\,\mathrm{d}p_{\mathrm{v}}/\mathrm{d}t$ it is clear that (3.14) reduces to (3.11) if $C\approx c$, $H\approx(p_B-p_\infty-p_{\mathrm{v}})/\rho_\infty$, and the term in C^{-2} is dropped. As it stands, (3.14) contains some second-order terms, although it is known (Jahsman 1968), and will be confirmed in II, that it is not accurate to second order. Nevertheless, according to some results of Hickling & Plesset (1964) and to our own preliminary calculations, it is found that (3.14) possesses a remarkable accuracy. Investigating the causes of this success we have realized that it is due to the use of the enthalpy directly, rather than the expansion (3.1). If, on the basis of (3.5b), one estimates $(p-p_\infty)/\rho_\infty$ to be of order u^2, the second term in this expansion appears to be of order Mach number squared, and therefore should be small. However, near the point of minimum radius, the correct order of $(p-p_\infty)/\rho_\infty$ is not set by the velocity squared, but rather by the first term of (3.5b), $\partial\varphi/\partial t$. This term is very large and use of h avoids this source of error. This problem can be considered from the point of view of the scaling of the equations, as will be done in II. For this reason we shall retain the enthalpy in the following developments.

4. Non-dimensional formulation

Let R_0 and U denote typical scales for the bubble radius and radial velocity. Then we introduce non-dimensional quantities, indicated by asterisks, as follows

$$\left.\begin{aligned} R=R_0R_*,\quad r=R_0r_*,\quad t=\frac{R_0}{U}t_*,\quad \varphi=R_0U\varphi_*,\\ h=U^2h_*,\quad c=c_\infty c_*,\quad p=p_\infty+\rho_\infty U^2p_*. \end{aligned}\right\} \quad (4.1)$$

At first sight this particular scaling is straightforward, although it conceals some subtle points which will be discussed in II. In terms of these variables, (2.4) and (2.5) become

$$\nabla_*^2\varphi_*+\frac{\epsilon^2}{c_*^2}\left(\frac{\partial h_*}{\partial t_*}+\frac{\partial\varphi_*}{\partial r_*}\frac{\partial h_*}{\partial r_*}\right)=0,\quad \frac{\partial\varphi_*}{\partial t_*}+\frac{1}{2}\left(\frac{\partial\varphi_*}{\partial r_*}\right)^2+h_*=0, \quad (4.2a,b)$$

where

$$\epsilon=\frac{U}{c_\infty} \quad (4.3)$$

is of the order of the bubble wall Mach number. Since the timescale is $T=R_0/U$, as

is clear from (4.1), this definition of ϵ coincides with the one previously given in (3.10). From (2.10) the enthalpy becomes

$$h_* = \frac{1}{\epsilon^2}\frac{c_*^2 - 1}{n-1}, \tag{4.4}$$

from which

$$c_*^2 = 1 + \epsilon^2(n-1)h_*. \tag{4.5}$$

The kinematic boundary condition (2.6) is

$$\frac{\partial \varphi_*}{\partial r_*} = \frac{\mathrm{d}R_*}{\mathrm{d}t_*} \quad \text{at } r_* = R_*, \tag{4.6}$$

while the dynamic one may be written

$$h_* = h_{B*} \quad \text{at } r_* = R_*, \tag{4.7}$$

where

$$h_{B*} = \frac{1}{\epsilon^2}\frac{1}{n-1}\left[\left(\frac{p_B + B}{p_\infty + B}\right)^{(n-1)/n} - 1\right],$$

with p_B given by (2.7).

The variable r_* defined in (4.1) is the appropriate coordinate in the near field. As discussed in the previous section, the appropriate coordinate in the far field is, instead, $r/c_\infty T$ or

$$\tilde{r} = \frac{r_*}{\epsilon}. \tag{4.8}$$

In terms of $\tilde{r}$ (4.2) are

$$\tilde{\nabla}^2 \varphi_* + c_*^{-2}\left(\frac{\partial h_*}{\partial t_*} + \epsilon^2 \frac{\partial \varphi_*}{\partial \tilde{r}}\frac{\partial h_*}{\partial \tilde{r}}\right) = 0, \quad \frac{\partial \varphi_*}{\partial t_*} + \tfrac{1}{2}\epsilon^2\left(\frac{\partial \varphi_*}{\partial \tilde{r}}\right)^2 + h_* = 0. \tag{4.9a,b}$$

Solutions of (4.2) and (4.9) are now sought in the form of power series in ϵ. The boundary conditions at infinity are imposed on the solutions of (4.9), while those at the bubble wall are imposed on the solution of (4.2). The remaining undetermined quantities can then be found by matching in the standard way (see, e.g., Van Dyke 1975).

5. Perturbation solution

For the inner equations (4.2), we let

$$\varphi_* = \varphi_0 + \epsilon\varphi_1 + \ldots, \quad h_* = h_0 + \epsilon h_1 + \ldots, \tag{5.1}$$

to find, at zero order,

$$\nabla_*^2 \varphi_0 = 0, \quad \frac{\partial \varphi_0}{\partial t_*} + \frac{1}{2}\left(\frac{\partial \varphi_0}{\partial r_*}\right)^2 + h_0 = 0, \tag{5.2a,b}$$

and at first order,

$$\nabla_*^2 \varphi_1 = 0, \quad \frac{\partial \varphi_1}{\partial t_*} + \frac{\partial \varphi_0}{\partial r_*}\frac{\partial \varphi_1}{\partial r_*} + h_1 = 0. \tag{5.3a,b}$$

For the outer equations (4.9), we let

$$\varphi_* = \phi_0 + \epsilon\phi_1 + \ldots, \quad h_* = H_0 + \epsilon H_1 + \ldots. \tag{5.4}$$

It follows from (4.5) that, up to order ϵ, c_* in (4.9a) can be taken as 1. Hence we find at zero order

$$\tilde{\nabla}^2 \phi_0 + \frac{\partial H_0}{\partial t_*} = 0, \quad \frac{\partial \phi_0}{\partial t_*} + H_0 = 0, \tag{5.5a,b}$$

with identical equations at first order

$$\tilde{\nabla}^2\phi_1+\frac{\partial H_1}{\partial t_*}=0, \quad \frac{\partial\phi_1}{\partial t_*}+H_1=0. \tag{5.6a,b}$$

The relevant solution of (5.2) has the form

$$\varphi_0=-\frac{f_0(t_*)}{r_*}+g_0(t_*), \quad h_0=\frac{f_0'}{r_*}-g_0'-\frac{1}{2}\frac{f_0^2}{r_*^4}, \tag{5.7a,b}$$

where here and in the following the prime indicates differentiation with respect to the argument. Imposing the kinematic boundary condition (4.6) one finds

$$f_0=R_*^2\,R_*'. \tag{5.8}$$

The solution of (5.5) such that both H_0 and $\partial\phi_0/\partial t_*$ vanish at infinity is

$$\phi_0=\tilde{r}^{-1}[F_0(t_*-\tilde{r})+G_0(t_*+\tilde{r})]+\alpha_0, \tag{5.9a}$$

$$H_0=-\tilde{r}^{-1}[F_0'(t_*-\tilde{r})+G_0'(t_*+\tilde{r})], \tag{5.9b}$$

where α_0 is a constant. For $\tilde{r}$ small, i.e. at the outer edge of the inner domain, (5.9a) is asymptotic to

$$\phi_0\sim\frac{F_0(t_*)+G_0(t_*)}{\epsilon r_*}+G_0'(t_*)-F_0'(t_*)+\alpha_0, \tag{5.10}$$

while for r_* large, which is the inner boundary of the outer domain, (5.7a) reduces to

$$\varphi_0\sim g_0(t_*). \tag{5.11}$$

The two solutions agree (i.e. match) in this domain where they are both valid provided that

$$F_0(t_*)=-G_0(t_*), \quad g_0(t_*)=2G_0'(t_*)+\alpha_0, \tag{5.12}$$

so that the final solution for the potential is

$$\varphi_0=-\frac{f_0(t_*)}{r_*}+2G_0'(t_*)+\alpha_0, \tag{5.13a}$$

$$\phi_0=\tilde{r}^{-1}[G_0(t_*+\tilde{r})-G_0(t_*-\tilde{r})]+\alpha_0, \tag{5.13b}$$

and for the enthalpy

$$h_0=\frac{f_0'}{r_*}-\frac{1}{2}\frac{f_0^2}{r_*^4}-2G_0''(t_*), \tag{5.14a}$$

$$H_0=\tilde{r}^{-1}[G_0'(t_*+\tilde{r})-G_0'(t_*-\tilde{r})]. \tag{5.14b}$$

The interpretation of these results is straightforward. To the present lowest order the outer fields are not affected by the presence of the bubble and the incident wave $G_0(t_*+\tilde{r})$ is reflected unaltered. In the inner field the superposition of the incident and reflected waves adds, to the perturbation caused by the bubble, a time-varying, spatially uniform component. In this sense the bubble 'sees' a uniform field at its 'infinity'.

The solution of the inner first-order equation (5.3a) for φ_1 is formally the same as (5.7a), but now the kinematic boundary condition requires $f_1(t_*)=0$, so that

$$\varphi_1=g_1(t_*), \quad h_1=-g_1'(t_*). \tag{5.15a,b}$$

The solution of the corresponding outer equations (5.6) is also formally identical to the zero-order one (5.9). However, we interpret the terms in ϵ as the correction to

the situation represented by (5.13*b*), (5.14*b*) introduced by the presence of the bubble. Hence ϕ_1, H_1 cannot contain incoming, but only outgoing waves, and therefore we write

$$\phi_1 = \tilde{r}^{-1}F_1(t_*-\tilde{r}), \quad H_1 = -\tilde{r}^{-1}F_1'(t_*-\tilde{r}). \tag{5.16a,b}$$

Since the combination of zero- and first-order terms approximates the exact solution with an error of order ϵ^2, the correct matching prescription is now

$$\lim_{r_*\to\infty} \epsilon^{-1}(\varphi_0+\epsilon\varphi_1) = \lim_{\tilde{r}\to 0} \epsilon^{-1}(\phi_0+\epsilon\phi_1), \tag{5.17}$$

rather than the one previously used. Applying this condition one finds

$$F_1(t_*) = -f_0(t_*), \quad g_1(t_*) = -F_1'(t_*) = f_0'(t_*), \tag{5.18}$$

so that

$$\varphi_1 = f_0'(t_*), \quad \phi_1 = -\tilde{r}^{-1}f_0(t_*-\tilde{r}). \tag{5.19a,b}$$

The enthalpy fields also satisfy (5.17) provided (5.18) hold. Combining (5.14*a*) and (5.15*b*) we find the following approximation to the liquid enthalpy valid near the bubble:

$$h_* = \frac{f_0'}{r_*} - \frac{1}{2}\frac{f_0^2}{r_*^4} - 2G_0'' - \epsilon f_0''' + O(\epsilon^2), \tag{5.20}$$

where all the functions in the right-hand side have argument t_* and f_0 is given by (5.8). With the results (5.14*a*) and (5.20) we can now derive approximate equations of motion for the bubble radius.

6. The equations of motion for the bubble radius

We shall now derive and comment on the equations of motion for the bubble radius valid to zeroth and first order in ϵ. In the first case we impose the dynamic boundary condition (4.7) on (5.14*a*) to obtain

$$\frac{f_0'}{R_*} - \frac{1}{2}\frac{f_0^2}{R_*^4} - 2G_0'' = h_{B*}, \tag{6.1}$$

or, using (5.8) to eliminate f_0,

$$R_* R_*'' + \tfrac{3}{2}R_*'^2 = h_{B*} + 2G_0''. \tag{6.2}$$

In dimensional variables this equation is

$$R\frac{\mathrm{d}^2R}{\mathrm{d}t^2} + \frac{3}{2}\left(\frac{\mathrm{d}R}{\mathrm{d}t}\right)^2 = h_B + 2U^2\frac{\mathrm{d}^2G_0}{\mathrm{d}t_*^2}(t_*). \tag{6.3}$$

To the present order of approximation, $h_B \simeq (p_B - p_\infty)/\rho_\infty$. With this, it is seen that (6.3) is identical to the Rayleigh–Plesset equation (3.12), provided that

$$p_v(t) = -2\rho_\infty U^2\frac{\mathrm{d}^2G_0}{\mathrm{d}t_*^2}. \tag{6.4}$$

It will be seen below that the use of h is preferable to that of the expansion (3.1) because it permits a better estimate of the energy radiated by the bubble. Equation (6.3) evidently completely fails to account for this phenomenon and therefore the use of h here is unwarranted since this equation can only be legitimately used when radiation losses are negligible anyway. From the point of view of the present perturbation solution the Rayleigh–Plesset equation is seen to have an error of order ϵ, i.e. of the order of the Mach number of the bubble-wall motion.

At the next order we use (5.20) to obtain

$$\frac{f_0'}{R_*}-\frac{1}{2}\frac{f_0^2}{R_*^4}-2G_0''-\epsilon f_0''=h_{B*} \tag{6.5}$$

If f_0'' is computed using (5.8), third-order derivatives of the radius appear, a problem which is well known in the classical theory of the electron (Jackson 1975; Rohrlich 1965; Burke 1970). This difficulty can be circumvented if it is realized that f_0, being multiplied by ϵ, can be evaluated from (6.1) maintaining an overall error of order ϵ^2 in (6.5). In this way we find

$$f_0''=\tfrac{1}{2}(R_*'^3+2R_*R_*'R_*'')+R_*'(h_B+2G_0'')+R_*(h_B'+2G_0''')+O(\epsilon), \tag{6.6}$$

and, upon substitution into (6.5),

$$(1-\epsilon R_*')R_*R_2''+\tfrac{3}{2}(1-\tfrac{1}{3}\epsilon R_*')R_*'^2=(1+\epsilon R_*')(h_{B*}+2G_0'')+\epsilon R\frac{\mathrm{d}}{\mathrm{d}t}(h_{B*}+2G_0''). \tag{6.7}$$

In dimensional variables this equation is, using (6.4),

$$\left(1-c_\infty^{-1}\frac{\mathrm{d}R}{\mathrm{d}t}\right)R\frac{\mathrm{d}^2R}{\mathrm{d}t^2}+\frac{3}{2}\left(1-\tfrac{1}{3}c_\infty^{-1}\frac{\mathrm{d}R}{\mathrm{d}t}\right)\left(\frac{\mathrm{d}R}{\mathrm{d}t}\right)^2$$
$$=\left(1+c_\infty^{-1}\frac{\mathrm{d}R}{\mathrm{d}t}\right)\left(h_B-\frac{p_\mathrm{v}}{\rho_\infty}\right)+\frac{R}{c_\infty}\frac{\mathrm{d}}{\mathrm{d}t}\left(h_B-\frac{p_\mathrm{v}}{\rho_\infty}\right). \tag{6.8}$$

In the expansion (3.1), the first correction to the approximation $h=(p-p_\infty)/\rho_\infty$ is of order ϵ^2, and therefore this approximation could, formally, be used in (6.8), thus recovering the Keller equation (3.11) to the extent that $p_\mathrm{v}(t+R/c_\infty)\approx p_\mathrm{v}(t)+(R/c_\infty)\,\mathrm{d}p_\mathrm{v}/\mathrm{d}t$. It will be shown below, however, that the form (6.8) with the enthalpy is slightly superior to the Keller form (3.11).

If, instead of proceeding as in (6.6), we had used (5.8) to compute f_0'' and then used the Rayleigh–Plesset equation (6.2) to evaluate R_*''', an equation of the Herring form (3.13) would have been found in place of (6.8). Thus, as had been anticipated, the two equations are exactly equivalent to order ϵ. More generally, if one writes $f_0''=\lambda f_0''+(1-\lambda)f_0''$ and uses (6.1) to evaluate the first term and (6.2) to express the third derivative of the radius which appears on expanding the second term, one finds

$$\left[1-(\lambda+1)c_\infty^{-1}\frac{\mathrm{d}R}{\mathrm{d}t}\right]R\frac{\mathrm{d}^2R}{\mathrm{d}t^2}+\frac{3}{2}\left[1-\tfrac{1}{3}(3\lambda+1)c_\infty^{-1}\frac{\mathrm{d}R}{\mathrm{d}t}\right]\left(\frac{\mathrm{d}R}{\mathrm{d}t}\right)^2$$
$$=\left[1+(1-\lambda)c_\infty^{-1}\frac{\mathrm{d}R}{\mathrm{d}t}\right]\left(h_B-\frac{p_\mathrm{v}}{\rho_\infty}\right)+\frac{R}{c_\infty}\frac{\mathrm{d}}{\mathrm{d}t}\left(h_B-\frac{p_\mathrm{v}}{\rho_\infty}\right). \tag{6.9}$$

The same result can be obtained by multiplying (6.3) by $(\lambda/c_\infty)\,\mathrm{d}R/\mathrm{d}t$ and subtracting the result from (6.8). The arbitrary parameter λ must, of course, be of smaller order than $1/\epsilon$ so as not to destroy the order of accuracy of the approximate equation.

We propose to refer to (6.9) as the *general Keller–Herring equation*. Any member of this one-parameter family of equations is *a priori* an acceptable form of the radial equation of motion correct to first order in the Mach number. Criteria for the selection of an optimal value of λ do not appear to be available and, as is made clear in II, even the consideration of the next equation, valid to order (Mach number)^2, gives no indication on this point. We examine the matter numerically in the next section.

In closing we offer, in the light of (6.9), some comments on the equations proposed in the literature. In the first place, the form obtained by replacing h_B with

$(p_B - p_\infty)/\rho_\infty$ is, as already stated, formally entirely equivalent to (6.9) (in the sense that both have error terms of order (Mach number)^2), and hence this is not an essential difference. With the exception of the work of Tomita & Shima (1977), the related one of Fujikawa & Akamatsu (1980), and the results of II, no equation accurate to order (Mach number)^2 exists. Therefore all equations in which terms multiplied by c_∞^{-2} appear are not correct to second order, and will be considered here only in their truncated form obtained by dropping such terms. In this sense the equation of Flynn (1975) reduces to the Keller form ($\lambda = 0$) and that of Rath (1980) to the Herring form (i.e. $\lambda = 1$). The equation of Gilmore (1952) (3.14) has already been considered in §3 and the same considerations apply to Cramer's (1980) adaptation of it to the case of forced motion. Tilmann (1980) has also derived an equation which, aside from terms in c_∞^{-2}, is identical with (6.8) including the use of the enthalpy rather than the pressure. No justification of this procedure is, however, given.

7. Numerical computations

The preceding analysis has led to a one-parameter family of equations all members of which are *a priori* legitimate approximations to the description of the radial dynamics of a bubble in a compressible liquid. No criteria seem to be available for the selection of any particular equation of the family and it has therefore been decided to examine the question by comparing with a few numerical simulations of the collapse process obtained by solving the original partial differential formulation of §2. The reason for choosing this particular process is that near the end of the collapse the pressure changes are greatest and the effect of compressibility most pronounced.

It is clear that the results derived from this comparison cannot be fully satisfactory, if only because they are necessarily limited to a few specific cases. Nevertheless, certain trends seem to emerge from the comparison which indicate that an equation close to the Keller form is slightly superior to others. Here we discuss the results. The numerical method is a standard version of the method of characteristics and is briefly described in the Appendix. Being based on the characteristics it fails when a shock wave forms in the liquid and accordingly the computation must be stopped shortly after the first point of minimum radius is reached and the cavity begins to rebound.

When the bubble starts from rest, a major portion of the time before the minimum radius is reached is spent in a state of very slow motion during which the velocity very gradually builds up. These conditions are such that the perturbation results are quite accurate to describe them. To save computer time we have therefore started the numerical simulation at a time $\bar{t}_* < 0$ using as initial conditions for the fields the analytic expressions to be given in full in II. In typical cases the values of the radius and radial velocity at the starting time $\bar{t}_*$ were of the order of 0.5 and -10 respectively. We have examined the error introduced by the use of the approximate analytic expressions in a few cases by starting the numerical calculation earlier or later and we have found negligible differences in the results.

We consider free oscillations, in which the bubble is released at the initial instant $t_* = 0$ with a radius greater than the equilibrium value and the ambient pressure stays constant, and forced oscillations in which the bubble, initially in equilibrium, is excited by an incoming pressure pulse.

To close the mathematical formulation it is necessary to specify the law of variation of the internal pressure p_i appearing in (2.7). The assumption that the liquid remains isothermal effectively uncouples the internal problem from the external one and this

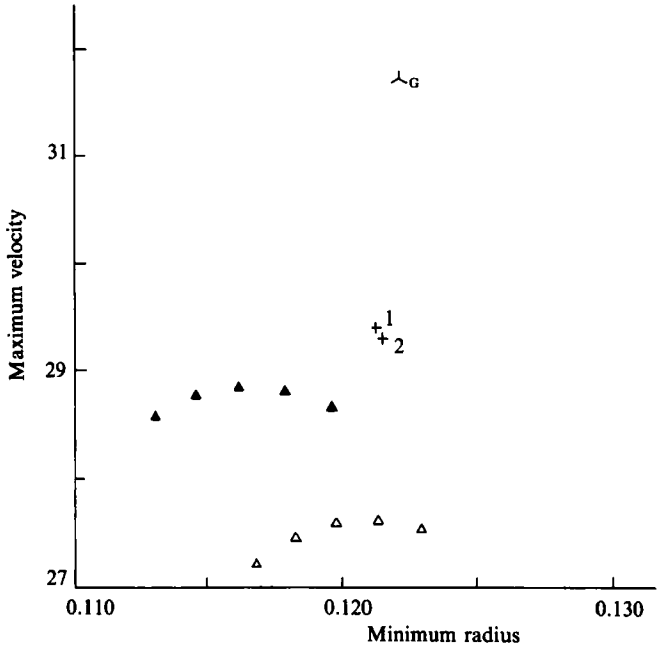

FIGURE 1. Dimensionless maximum velocity attained during the first rebound versus the dimensionless minimum radius at the end of the preceding collapse, which is completed at a dimensionless time close to 3.68. The filled triangles are the results obtained from (6.9), the open triangles are the corresponding results obtained from the same equation written in terms of the pressure rather than the enthalpy, i.e with $(p_B - p_\infty)/\rho_\infty$ in place of h_B. The symbol marked G is the result given by the Gilmore equation (3.14). The values of the parameter λ appearing in the equation are, from left to right, 1 (Herring form), 0.75, 0.5, 0.25, 0 (Keller form). The crosses are the results given by the numerical calculation with the method of characteristics starting from $t_* = 3.6653$, $R_* = 0.5522$, $R'_* = -14.26$ and using a spatial grid with 400 nodes (point 1) and from $t_* = 3.6250$, $R_* = 0.9322$, $R'_* = -6.863$ with 250 nodes (point 2). In both cases $\beta = 4$, $\Delta x = 0.005$. Initial radius $R_*(0) = 4$.

quantity could in principle be computed by solving the conservation equations in the bubble (see, e.g., Prosperetti, Crum & Commander 1986). For the present purposes of comparison, however, a simpler procedure is adequate and we assume an adiabatic pressure–volume relation,

$$p_i = p_{i0}\left(\frac{R_0}{R}\right)^{3\gamma}, \tag{7.1}$$

where R_0 is the equilibrium radius, p_{i0} the corresponding internal pressure, and γ the ratio of the specific heats. The equilibrium radius is given by (see, e.g., Plesset & Prosperetti 1977)

$$R_0 = \frac{2\sigma}{p_{i0} - p_\infty}. \tag{7.2}$$

This quantity is used as the unit of length in the presentation of the results. The unit of velocity is taken as

$$U = \left(\frac{p_\infty}{\rho_\infty}\right)^{\frac{1}{2}}. \tag{7.3}$$

Furthermore we take $B = 3049.13$ bars, $n = 7.15$ in the equation of state of the liquid, (2.8). The other pertinent numerical values are $\gamma = 1.4$, $p_\infty = 1$ bar,

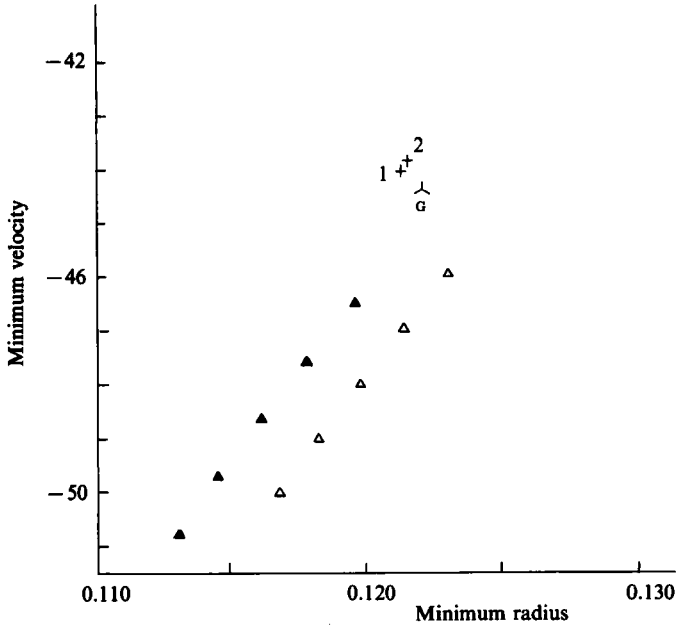

FIGURE 2. Minimum dimensionless negative velocity (maximum in absolute value) reached by the bubble wall during the first collapse versus the dimensionless minimum radius at the end of the collapse. The triangles correspond, in ascending order, to $\lambda = 1$ (Herring), 0.75, 0.5, 0.25, 0 (Keller). Other symbols as in figure 1.

$\rho_\infty = 0.998$ g/cm^3, $\mu = 0.01$ poise, $\sigma = 72.5$ erg/cm^2, $R_0 = 0.01$ cm. It may be noted that, when R_0 is not too small, as in the present case, the mathematical formulation can be shown to be approximately independent of this quantity after a suitable scaling.

In the collapse the most critical sequence of events takes place near the point of minimum radius. It is here that the internal pressure reaches very high values and the elastic energy, which will subsequently be radiated away to infinity, is stored in the liquid. To get a clearer picture of the differences among the equations, rather than showing portions of the $R_*(t_*)$ curves in this region, which are all very close together, we have chosen to single out three critical quantities and to show their variation with the parameter λ appearing in the generalized Keller–Herring equation (6.9). The first one is the minimum velocity (maximum in absolute value) reached during the collapse, the second one is the minimum radius, and the third one is the maximum velocity during the first rebound, which is reached very shortly after the point of minimum radius. The last quantity, in particular, gives a very clear indication of the radiation losses from the bubble.

Figures 1–3 refer to the case of free oscillations for an initial radius equal to 4 times the equilibrium value. Figure 1 shows the maximum velocity reached during the first rebound plotted as a function of the minimum radius for different values of λ. The two crosses are the results obtained with the method of characteristics for two different starting times $\bar{t}_*$ of the integration. In one case the initial values of the radius and radial velocity were 0.5522 and -14.26, respectively, and in the second case 0.9322 and -6.863. We include both results to given an idea of the range of variation with the initial conditions. The open triangles are the prediction of the generalized Keller–Herring equation in terms of the pressure while the full triangles are the

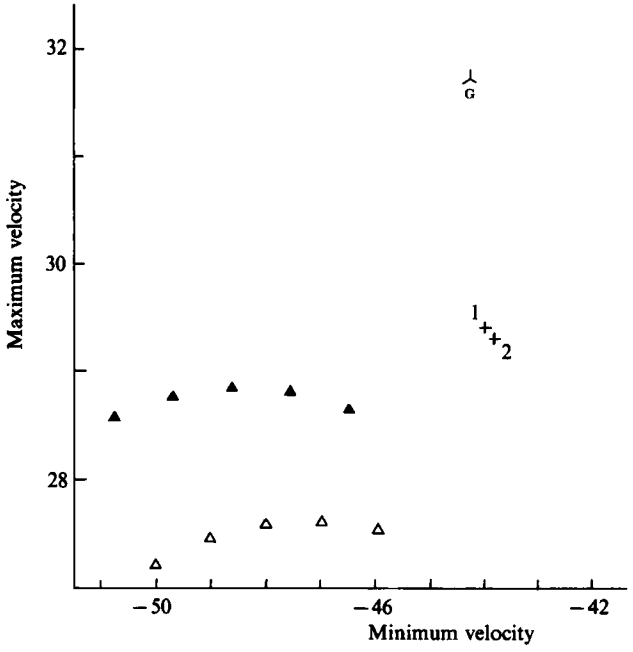

FIGURE 3. Cross-plot of the dimensionless maximum velocity during the first rebound of figure 1 versus the dimensionless minimum velocity (maximum in absolute value) during the first collapse of figure 2. The triangles are, from left to right, for $\lambda = 1$ (Herring), 0.75, 0.5, 0.25, 0 (Keller). Other symbols as in figure 1.

predictions in terms of the enthalpy. In both cases the far-right points correspond to $\lambda = 0$ (i.e. the Keller form), and the far-left ones to $\lambda = 1$ (i.e. the Herring form). The intermediate points are for $\lambda = 0.25$, 0.5, 0.75 in this order from right to left. The last symbol marked G is the prediction of the Gilmore equation (3.14). Figure 2 is a plot of the minimum velocity versus the minimum radius. Since this velocity is negative, this is actually in absolute value the largest velocity attained during the whole process. In the units used here the speed of sound is $c_\infty/U = 147.67$, and therefore it is seen that the maximum Mach number reached is of the order of 0.3. Here the uppermost points are for $\lambda = 0$ and the bottom ones for $\lambda = 1$. Finally, figure 3 is a cross-plot of the preceding two figures showing the maximum versus the minimum velocity.

In spite of the not too large value of the Mach number, the case to which the figures refer is already rather extreme because the maximum pressure reached in the bubble is of the order of 7000 bars. For this reason the equations in terms of the enthalpy are seen to perform globally better than those in terms of the pressure, as had been anticipated (see especially figures 1 and 3). Clearly, in these conditions the series expansion (3.1) is a very poor approximation to the correct pressure–enthalpy relation. The large value of the pressure in spite of a relatively small Mach number is an illustration of the point already made about the relative importance of the terms $\partial\varphi/\partial t$ and $\frac{1}{2}u^2$ of the Bernoulli equation (2.5) in these circumstances.

For all the quantities plotted in figures 1–3 the Keller form of the equation is seen to be superior to the Herring one. Furthermore, there does not seem to be anything to gain by using values of λ outside the interval 0–1. This has been confirmed by some trial calculations conducted with λ in the range 0 to -2. The Gilmore equation is

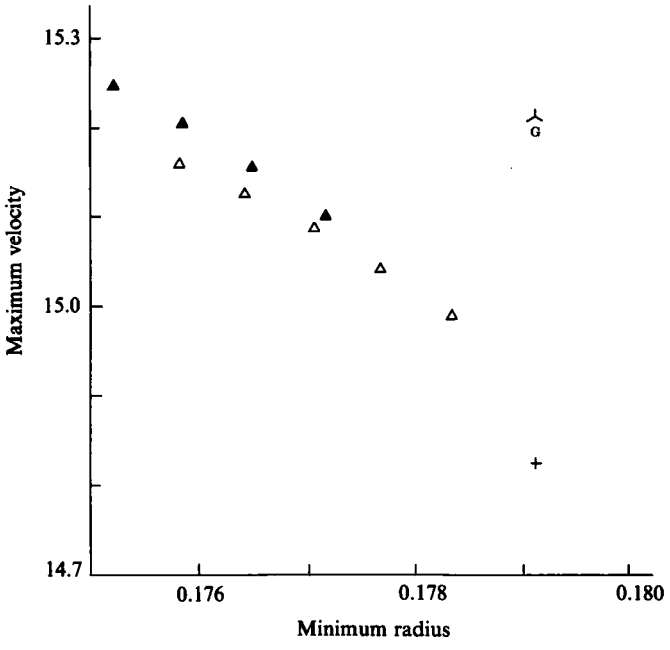

FIGURE 4. Same as figure 1 but for $R_*(0) = 3$. The filled triangles ((6.9) in terms of the enthalpy) are, from left to right, for $\lambda = 0.75, 0.5, 0.25, 0$ (Keller). The open ones ((6.9) in terms of the pressure) are, in the same order, for $\lambda = 1$ (Herring), 0.75, 0.5, 0.25, 0 (Keller). The cross is the result of the method of characteristics applied with 200 nodes, $\beta = 4$, $\Delta x = 0.005$, starting from $R_* = 0.8458$, $R'_* = -5.016$.

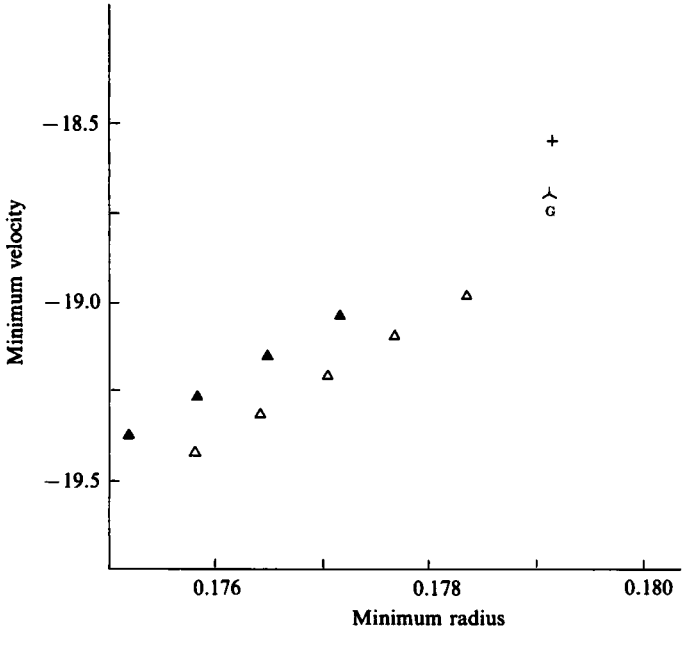

FIGURE 5. Same as figure 2 but for $R_*(0) = 3$. The points, in ascending order, are for the values of λ as in figure 4.

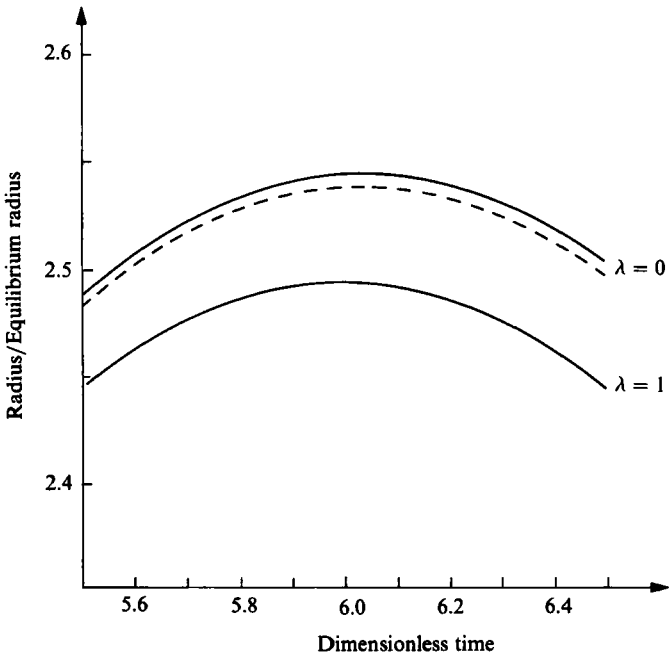

FIGURE 6. Portion of the dimensionless radius-versus-time curve near the maximum attained during the first rebound for an initial value of the radius $R_*(0) = 4$. The lowest curve is the result of (6.9) with $\lambda = 1$ (Herring form) in terms of the enthalpy. The upper line is for $\lambda = 0$ (Keller form) in terms of the enthalpy. The middle line is for $\lambda = 0$ with the equation written in terms of the pressure.

in excellent agreement with the numerical results in figure 2, but is seen to be clearly inferior to the Keller equation in figures 1 and 3.

Figures 4 and 5 are analogous to 1 and 2 for an initial radius equal to 3 times the equilibrium value. In this case the maximum Mach number is about 0.13 and the maximum internal pressure 1700 bars. Hence one expects a smaller difference between the equations in terms of the enthalpy and of the pressure, which is confirmed by the results. Otherwise the Keller form is found also in this case to be superior to the Herring one.

In figure 6 we show a portion of the radius–time curve predicted by the approximate differential equations near the maximum after the first collapse. The height of this maximum is sensitive to the amount of acoustic energy lost by radiation and hence we can see that the Herring form ($\lambda = 1$, equation in terms of the pressure, lowest curve) tends to give a stronger radiation loss than the Keller form ($\lambda = 0$, upper two curves; the dotted one in terms of the pressure and the continuous one in terms of the enthalpy). It will be seen in II that the second-order equations predict slightly higher radii. The energy lost by radiation is thus seen to be overpredicted by the first-order equations, especially if the pressure is used in place of the enthalpy. It may be noted that the maximum radius predicted by the incompressible Rayleigh–Plesset equation for this case is essentially the same as the initial one, i.e. $R_M = 4$, while that in figure 6 is about 2.55. Since the energy of the system can be taken to be proportional to R_M^3 to a first approximation, it is seen that, in this case, approximately 74% of the initial energy is lost by radiation during the first compression and expansion cycle.

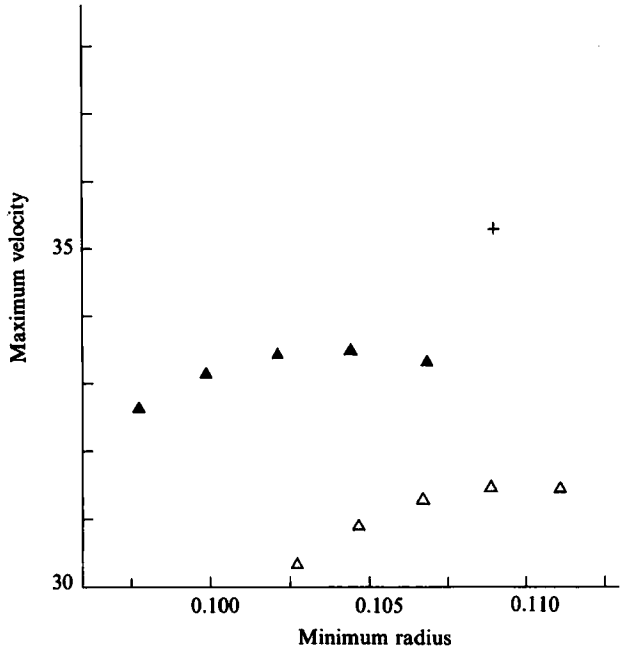

FIGURE 7. Same as figure 1 for the forced case in which the incident wave has the form given by (7.5) and the bubble radius initially has the equilibrium value $R_*(0) = 1$. The cross is the result obtained with the method of characteristics starting from $R_* = 0.99999$, $R'_* = -0.417 \times 10^{-4}$ with 250 nodes, $\beta = 4$, $\Delta x = 0.005$.

To analyse a case of forced oscillations we have considered a Gaussian pulse as seen in the inner field, i.e.

$$2G''_0(t_*) = A \exp\left[-\frac{(t_*-t_0)^2}{2\tau^2}\right], \tag{7.4}$$

where A, τ, t_0 are constants. Upon integration one has

$$G_0 = \frac{(2\pi)^{\frac{1}{2}}}{4} A\tau(t_*-t_0)\,\mathrm{erf}\left(\frac{t_*-t_0}{\tau\sqrt{2}}\right) + \tfrac{1}{2}A\tau^2 \exp\left[-\frac{(t_*-t_0)^2}{2\tau^2}\right]. \tag{7.5}$$

It was found on trial runs that, if τ is large, the bubble is compressed quasi-statically, which is a situation of little interest here. For moderate values of τ (around 1) the compression is non-monotonic. Since the rebound phase cannot be followed with our numerical method, this situation is also not suitable to carry out a comparison between numerical and perturbation results. Upon further reduction of the value of τ the behaviour becomes closer to a strong monotonic compression, followed by a rebound and damped oscillations. For this reason we have taken $\tau = 0.01$. In order to achieve a sufficiently violent compression we have also taken $A = -300$. The parameter t_0 has been chosen so that at the initial instant the pressure in the vicinity of the bubble differs negligibly from the undisturbed pressure. The value $t_0 = 0.44766$ has been used in this example.

We show in figures 7–9 the same type of information as in figures 1–3 for this case of forced oscillations. As before the filled symbols indicate results obtained with the equations in terms of the enthalpy and the open ones in terms of the pressure. The

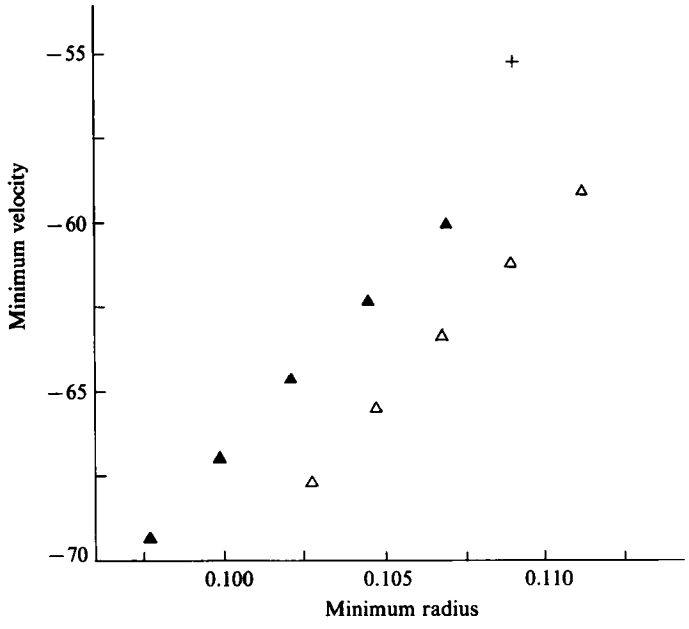

FIGURE 8. Minimum dimensionless velocity versus minimum dimensionless radius for the forced case of figure 7.

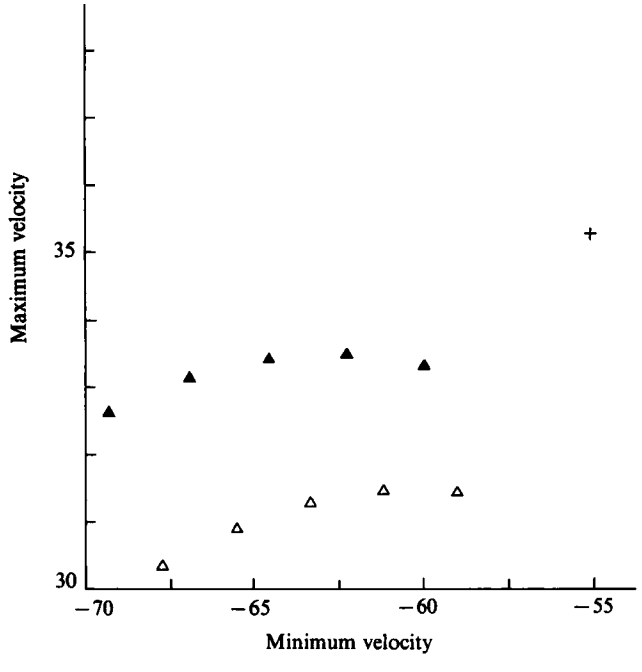

FIGURE 9. Maximum dimensionless velocity versus minimum dimensionless velocity for the forced case of figure 7.

general appearance of these figures is quite similar to the preceding ones and the same conclusions apply.

Further comparisons, including the second-order equations, will be found in II.

The present study has been supported in part by the Courant Institute of Mathematics, New York University, through the grant ONR N00014-81-K-0002.

Appendix. Numerical method

In the numerical solution of the present problem there are two basic difficulties. In the first place, the position of the boundary varies with time. Secondly, the spatial scale to be resolved gets progressively smaller as the collapse proceeds. Thus, if a fixed grid is adopted, an excessively large number of points is required. To avoid both problems we introduce a new spatial variable according to

$$x = \left[\frac{r}{R(t)}\right]^{1/\beta}. \tag{A 1}$$

Since

$$\frac{\mathrm{d}r}{\mathrm{d}x} = \beta r^{(\beta-1)/\beta} R^{1/\beta}, \tag{A 2}$$

for $1 < \beta$ this transformation has the further advantage that, in terms of the original variable r, nodes progressively further apart from each other correspond to an equispaced grid in x.

In terms of x, (2.1) and (2.2) become, in characteristic form,

$$\frac{\mathrm{d}u}{\mathrm{d}t} \pm \frac{\mathrm{d}P}{\mathrm{d}t} \pm \frac{2cu}{Rx^{\beta}} = 0, \tag{A 3}$$

along the characteristic lines $C_{\pm}$ defined by

$$\frac{\mathrm{d}x^{\beta}}{\mathrm{d}t} = R^{-1}(u - x^{\beta}R' \pm c). \tag{A 4}$$

The quantity P is defined by

$$P = \int_{p_{\infty}}^{p} \frac{\mathrm{d}p}{\rho c}, \tag{A 5a}$$

and, with (2.8), has the explicit expression

$$P = \frac{2n}{n-1}\left[\frac{p_{\infty}+B}{n\rho_{\infty}}\right]^{\frac{1}{2}}\left[\left(\frac{p+B}{p_{\infty}+B}\right)^{(n-1)/2n} - 1\right]. \tag{A 5b}$$

We illustrate the numerical method with reference to figure 10. Suppose the solution is known up to time t^n. To determine it at time t^{n+1} we use the trapezoidal rule and write

$$u_j^{n+1} - u_{\pm} + P_j^{n+1} - P(A_{\pm}) \pm \tfrac{1}{2}\Delta t[H_j^{n+1} + H(A_{\pm})] = 0, \tag{A 6}$$

$$x_j^{\beta} - (x_{\pm})^{\beta} - \tfrac{1}{2}\Delta t[Q^{(\pm)}(A) + Q^{(\pm)}(A_{\pm})] = 0, \tag{A 7}$$

where subscripts and superscripts denote spatial and temporal locations and

$$Q^{(\pm)} = R^{-1}(u - x^{\beta}R' \pm c). \tag{A 8}$$

The points $A_{\pm}$ are the intersections of the $C_{\pm}$ characteristics with the line $t = t^n$ and are given by (A 7). The values of u and p at $x_{\pm}$ are obtained by quadratic interpolation

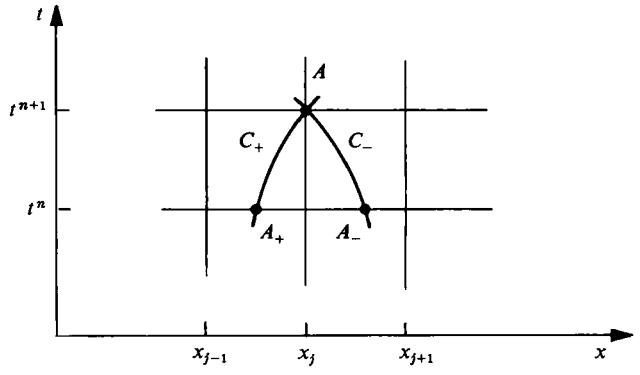

FIGURE 10. Illustration of the numerical method.

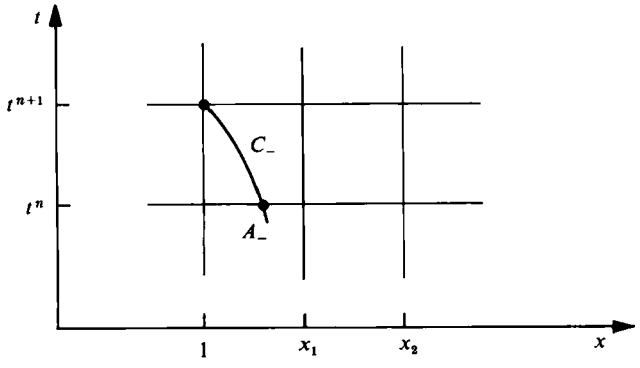

FIGURE 11. Modification of the boundaries of the computational domain: the left boundary.

using the known values at x_j, $x_{j\pm1}$. The four equations (A 6), (A 7) are a closed system in the four unknowns $x_\pm$, u_j^{n+1}, P_j^{n+1}, the solution of which is readily obtained by an iterative procedure such as the Newton–Raphson method.

This basic approach must be suitably modified at the boundaries of the computational domain. For the left boundary, $x_0 = 1$, we can only use the information propagating along the C_- characteristic (figure 11), but we also know from the kinematic boundary condition that $u(x = 1, t^{n+1}) = (R')^{n+1}$ and, from the dynamic one, that

$$p(x = 1, t^{n+1}) = p_{i0}\left(\frac{R_0}{R^{n+1}}\right)^{3\gamma} - \frac{2\sigma + 4\mu(R')^{n+1}}{R^{n+1}}. \tag{A 9}$$

Furthermore, again using the trapezoidal rule,

$$R^{n+1} = R^n + \tfrac{1}{2}\Delta t[(R')^{n+1} + (R')^n]. \tag{A 10}$$

Using this relation the two C_- equations (A 6), (A 7) and (A 9) can be converted into a nonlinear system for the three unknowns x_-, $(R')^{n+1}$, $p(x = 1, t^{n+1})$ which is again solved iteratively. The value of p_- is obtained by quadratic interpolation using the points x_0, x_1, x_2.

At the right boundary $x = x_N$, which is the 'infinity' of the computational domain,

use can be made only of the C_+ characteristics. To obtain a closed system we add the Euler equation in linearized form

$$\frac{\partial u}{\partial t} = -\rho_\infty \frac{\partial p}{\partial r},$$

which, discretized and written in terms of x, becomes

$$[(R')^{n+1}(u_N^{n+1} - u_{N-1}^{n+1}) - x_N^{-\beta}\rho_\infty^{-1}(p_N^{n+1} - p_{N-1}^{n+1})]\frac{\Delta t}{\Delta x} - \beta x_N^{-1} R^{n+1}(u_N^{n+1} - u_N^n) = 0.$$

In the numerical procedure the values u_{N-1}^{n+1}, p_{N-1}^{n+1} are computed before the last node is considered and hence this equation effectively contains the only unknowns u_N^{n+1}, p_N^{n+1}. The C_+ relation (A 6) introduces the further unknown x_+, and the C_+ relation (A 7) closes the system, which is also solved iteratively. The values of u_+, p_+ are obtained by quadratic interpolation using x_N, x_{N-1}, x_{N-2}.

The integration has been performed with a variable time step chosen according to the rule

$$t^{n+1} - t^n = \frac{C\Delta x}{\beta x^{1-\beta} \max\limits_{1 \leqslant j \leqslant N} (|Q_j^{(+)}|, |Q_j^{(-)}|)}.$$

For the Courant number C the value $\frac{1}{2}$ has been used in most of the calculations. For the other parameters, typical values used are $\beta = 4$, $N = 200$–400, $\Delta x = 5 \times 10^{-3}$. The computer program has been successfully tested by applying it to the collapse of a one-dimensional bubble for which an analytic solution is available (Biasi, Prosperetti & Tozzi 1972).

REFERENCES

Biasi L., Prosperetti, A. & Tozzi, A. 1972 Collapse of one-dimensional cavities in compressible liquids. *Phys. Fluids* **15**, 1848–1850.

Burke, W. L. 1970 Runaway solutions: remarks on the asymptotic theory of radiation damping. *Phys. Rev.* A **2**, 1501–1505.

Cole, R. H. 1948 *Underwater Explosions*. Princeton University Press, reprinted by Dover 1965.

Cramer, E. 1980 The dynamics and acoustic emission of bubbles driven by a sound field. In *Cavitation and Inhomogeneities in Underwater Acoustics* (ed. W. Lauterborn). Springer.

Epstein, D. & Keller, J. B. 1971 Expansion and contraction of planar, cylindrical, and spherical underwater gas bubbles. *J. Acoust. Soc. Am.* **52**, 975–980.

Flynn, H. G. 1975 Cavitation dynamics I. A mathematical formulation. *J. Acoust. Soc. Am.* **57**, 1379–1396.

Fujikawa, S. & Akamatsu, T. 1980 Effects of the non-equilibrium condensation of vapour on the pressure wave produced by the collapse of a bubble in a liquid. *J. Fluid Mech.* **97**, 481–512.

Gilmore, F. R. 1952 The collapse and growth of a spherical bubble in a viscous compressible liquid. *California Institute of Technology Hydrodynamics Laboratory, Rep. No.* 26-4.

Herring, C. 1941 Theory of the pulsations of the gas bubble produced by an underwater explosion. *OSRD Rep. No.* 236.

Hickling, R. & Plesset, M. S. 1964 Collapse and rebound of a spherical bubble in water. *Phys. Fluids* **7**, 7–14.

Jackson, J. D. 1975 *Classical Electrodynamics*, 2nd edn. Wiley.

Jahsman, W. E. 1968 Collapse of a gas-filled spherical cavity. *Trans. ASME* E: *J. Appl. Mech.* **35**, 579–587.

Keller, J. B. & Kolodner, I. I. 1956 Damping of underwater explosion bubble oscillations. *J. Appl. Phys.* **27**, 1152–1161.

KELLER, J. B. & MIKSIS, M. 1980 Bubble oscillations of large amplitude. *J. Acoust. Soc. Am.* **68**, 628–633.

KIRKWOOD, J. G. & BETHE, H. A. 1942 The pressure wave produced by an underwater explosion. *OSRD Rep. No.* 558.

LASTMAN, G. J. & WENTZELL, R. A. 1979 Cavitation of a bubble in an inviscid compressible liquid. *Phys. Fluids* **22**, 2259–2266.

LASTMAN, G. J. & WENTZELL, R. A. 1981 Comparison of five models of spherical bubble response in an inviscid compressible liquid. *J. Acoust. Soc. Am.* **69**, 638–642.

LAUTERBORN, W. 1983 Cavitation noise and its relation to cavitation bubble dynamics. Presented at the *5th US-GE-Hydroacoustics Symp. Horst Merbt-Symposium. Hamburg, June 13.*

LAUTERBORN, W. 1985 Acoustic chaos. In *Frontiers in Physical Acoustics.* (ed. D. Sette). Proceedings of the International School of Physics 'Enrico Fermi'. Academic.

LAUTERBORN, W. & SUCHLA, E. 1984 Bifurcation superstructure in a model of acoustic turbulence. *Phys. Rev. Lett.* **53**, 2304–2307.

LAUTERBORN, W. & VOGEL, A. 1984 Modern optical techniques in fluid mechanics. *Ann. Rev. Fluid Mech.* **16**, 223–244.

LEZZI, A. & PROSPERETTI, A. 1986 Bubble dynamics in a compressible liquid. II. Second-order theory. *J. Fluid Mech.* (submitted).

PLESSET, M. S. & PROSPERETTI, A. 1977 Bubble dynamics and cavitation. *Ann. Rev. Fluid Mech.* **9**, 145–185.

PROSPERETTI, A., CRUM, L. A. & COMMANDER, K. W. 1986 Nonlinear bubble dynamics. *J. Acoust. Soc. Am.* (in press).

RATH, H. J. 1980 Free and forced oscillations of spherical gas bubbles and their translational motion in a compressible fluid. In *Cavitation and Inhomogeneities in Underwater Acoustics* (ed. W. Lauterborn). Springer.

ROHRLICH, F. 1965 *Classical Charged Particles.* Addison-Wesley.

TILMANN, P. M. 1980 Nonlinear sound scattering by small bubbles, In *Cavitation and Inhomogeneities in Underwater Acoustics* (ed. W. Lauterborn). Springer.

TOMITA, Y. & SHIMA, A. 1967 On the behaviour of a spherical bubble and the impulse pressure in a viscous compressible liquid. *Bull. JSME* **20**, 1453–1460.

TRILLING, L. 1952 The collapse and rebound of a gas bubble. *J. Appl. Phys.* **23**, 14–17.

VAN DYKE, M. 1975 *Perturbation Methods in Fluid Mechanics*, annotated Edition. Parabolic.

WHITHAM, G. B. 1974 *Linear and Nonlinear Waves.* Wiley.